Escola de Primavera de Transição e Turbulência
Blumenau 2020

ABCM Associação Brasileira de Engenharia e Ciências Mecânicas

12th Spring School on Transition and Turbulence
September 21st-25th, 2020, Blumenau, SC, Brazil

EPTT-2020-0125
MEAN AND FLUCTUATING PRESSURE DISTRIBUTION CAUSED BY A TURBULENT WIND ON A STORAGE SILO

Adrián Roberto Wittwer
Facultad de Ingeniería, Universidad Nacional del Nordeste, Argentina.
a_wittwer@yahoo.es

Héctor Darío Mónaco
Universidad Tecnológica Nacional, FRRa, Argentina.
hectordariomonaco@gmail.com

Jorge Omar Marighetti
Facultad de Ingeniería, Universidad Nacional del Nordeste, Argentina.
jomarighetti@gmail.com

Hugo Félix Begliardo
Universidad Tecnológica Nacional, FRRa, Argentina.
hugo.begliardo@frra.utn.edu.ar

Mario Eduardo De Bortoli
Facultad de Ingeniería, Universidad Nacional del Nordeste, Argentina.
mdebortoli@yahoo.com.ar

Juan José Nittmann
Universidad Tecnológica Nacional, FRRa, Argentina.
juannittmann@hotmail.com

Acir Mércio Loredo Souza
Laboratorio de Aerodinâmica das Construções, Universidade Federal de Rio Grande do Sul, Brasil.
acir@ufrgs.br

Abstract. *Storage silos installations are very common in the agricultural areas of Argentina and Brazil. Accidents caused by the action of the wind on the structural components of silos are usually reported. For this reason, the UTN - Regional Rafaela and the Laboratorio de Aerodinámica of the UNNE began to develop experimental studies in a wind tunnel with the objective of analyzing the external pressure distribution on isolated silos and complementing the procedures established in the Argentine Wind Code CIRSOC 102 and in the Brazilian Code NBR 6123. The tests were carried out in the UNNE "Jacek P. Gorecki" wind tunnel, which is a boundary layer tunnel of the Eiffel-type. The total length of the tunnel is 39.65 m, the test section is 2.4 m wide × 1.8 m high × 22.8 m long and an axial fan generates a maximum speed of 25 m/s. Turbulence generators and surface roughness elements were used to simulate atmospheric wind and then a 1:100 scale model of the silo was tested. In this work, results of mean and fluctuating pressure values obtained by wind tunnel tests are presented. The turbulent wind actions defined by the fluctuating pressures are evaluated through the distributions of RMS and peak values.*

Keywords: *Aerodynamic forces, wind tunnel, Reynolds number.*

1. INTRODUCTION

The Argentine wind code CIRSOC 102 (INTI, 2001) and the Brazilian standard NBR 6123 (ABNT, 1988) establish the test conditions to apply the wind tunnel procedure to calculate the aerodynamic actions. Both codes indicate that the wind load coefficients obtained by wind tunnel tests under these conditions can replace the empirical coefficients indicated by the wind code. These conditions include the physical simulation of the atmospheric boundary layer (De Bortoli *et al.*, 2002), the similarity of the turbulence characteristics, the geometric similarity of the structure model, the minimum blockage conditions, the minimum longitudinal pressure gradient in the test section, the effects of Reynolds number and the response characteristics of the laboratory measurement instruments.

This work specifically refers to the experimental analysis of the effects of wind on agricultural storage silos through wind tunnel tests. A description of the reduced scale modeling technique is presented. A set of measurements on an isolated silo model is analyzed including the effects of roughness and Reynolds number.

The analysis of results includes values of the coefficients of average pressure, RMS, maximum and minimum peaks. The main objective of the work is to introduce fluctuating pressures in the wind load analysis of these metallic structures. The next step in this research is to extend the wind tunnel tests to grouped silos as they normally appear in agricultural establishments.

2. CHARACTERISTICS OF STORAGE SILOS

Cylindrical metal silos are widely used in Argentina, Uruguay and Brazil for grain storage due to their efficiency, cost and relative ease of assembly. Flat silos are generally built with corrugated metal sheets fixed to each other to guarantee the continuity of the cylindrical shell. The external configuration of flat-type silos is shown in Figure 1. The same figure (center) shows two silos after an accident caused by the wind in the southwest of Chaco (Argentina). Another picture, on the right, shows a wind accident in a group of silos near the RS-463 route in Rio Grande do Sul (Brazil).

Figure 1. Typical external configuration of flat silos and pictures showing silos after accidents caused by the wind.

The flow around a grain storage silo can be approximated to the flow around a cylinder. The flat silo to be analyzed in this work has a height-diameter ratio H/D = 2 considering a prototype of 16 m in diameter and 32 m in height. It is made up of a cylindrical metal structure and a conical roof. It has large dimensions in relation to the own weight so, from the aerodynamic point of view, it is susceptible to the problem of instability due to compression and overturning caused by the action of the wind.

3. EXPERIMENTAL ARRANGEMENTS

A description of the experimental research work is carried out in this section. First, some details of the "Jacek P. Gorecki" wind tunnel of the Universidad Nacional del Nordeste (UNNE) are presented, as well as the main characteristics of the incident turbulent wind. Then, the description of the silo scale model and the measurement system used is made.

3.1 Characteristics of the UNNE wind tunnel

The "Jacek P. Gorecki" wind tunnel of the UNNE (Figure 2) is an open-circuit boundary layer tunnel (Wittwer and Möller, 2000). The test section is 2.4m wide × 1.8m high × 22.8m long. The tunnel has two 1.2 m diameter rotating test tables; the table I at 3.8 m from the beginning of the chamber and the table II at 19.4 m. A 2.25 m diameter axial fan produces a maximum mean speed of 25 m/s at table II and the wind speed can be modified through a mechanical regulator. The fan is driven by a 92 kW electric motor at 720 rpm and a diffuser decelerates the air before leaving the wind tunnel.

This type of facility is classified like a low velocity atmospheric boundary-layer wind tunnel and it was built with the aim to perform aerodynamic studies of structural models. The atmospheric boundary layer is generally reproduced with help of surface roughness elements and vortex generators. Conditions of zero pressure gradient boundary layers can be obtained by means of a vertical displacement mechanism of the tunnel roof.

3.2 Turbulent incident flow

The turbulent boundary layer flow in the test section was performed by means of the Standen technique (1972). A part-depth simulation with vertical velocity distribution corresponding to a class I terrain was used for the wind tunnel tests. This type of terrain is designed as rural zone according to the Argentine wind code CIRSOC 102 and the Brazilian standard NBR 6123.

The power law for the vertical velocity distribution is of good application in neutral stability conditions of strong winds, typical for structural analysis. The value for the power law exponent is approximately 0.11 for a class I terrain. A partial boundary-layer thickness was simulated by means of two spire type generators and prismatic roughness elements placed on the test section floor (Figure 3).

Experimental values of the vertical profile of mean velocity and turbulence intensity obtained by means of this hardware simulation are shown in the Figure 3 (right). The reference mean speed during the measurements of these vertical profiles was 20.10 m/s. Experimental data were compared with the theoretical velocity profile and with empirical turbulence intensity profiles indicated in the NBR6123 (Blessmann, 1995).

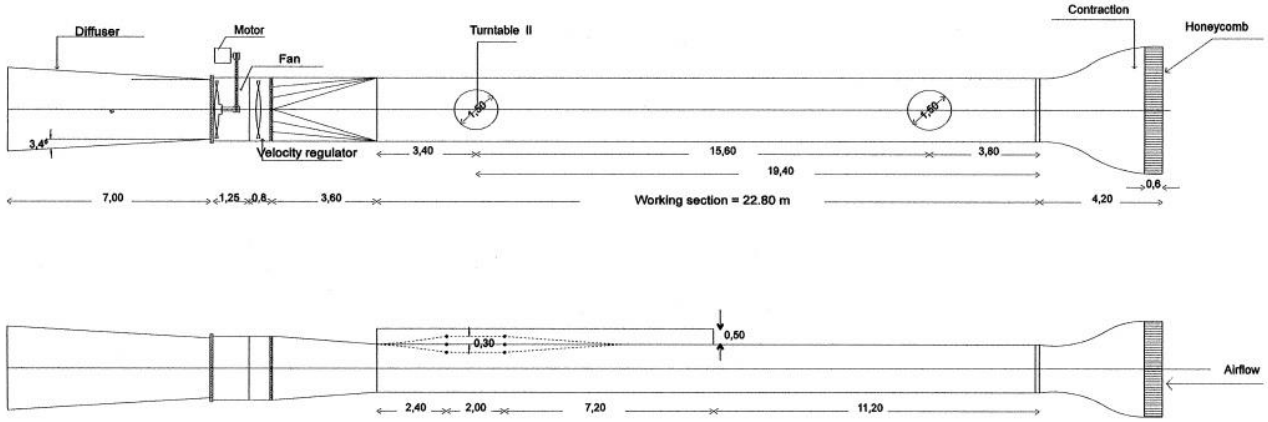

Figure 2. Prof. Jacek Gorecki Wind Tunnel – UNNE [m].

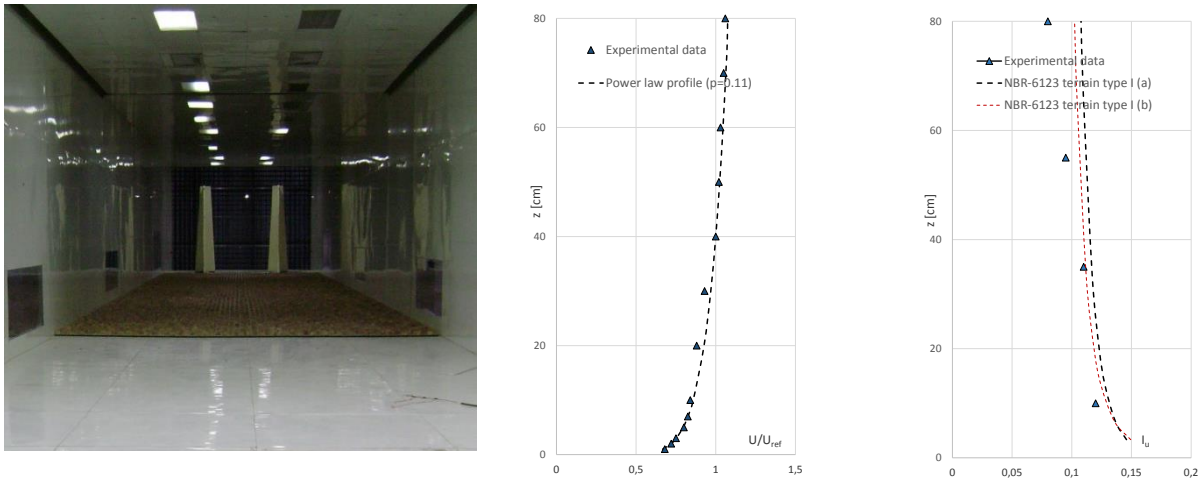

Figure 3. Hardware of turbulent flow simulation and vertical profiles of mean velocity and turbulence intensity.

3.3 Silo scale model

Two rigid models of the silo with a geometric scale of 1:100 were constructed; a smooth surface model and a rough surface model. The scale model is compatible with the scale factor of the simulation of the atmospheric wind obtained in the tunnel and aerodynamic relevance details were considered for modeling (Figures 4 and 5). The roughness elements of the model were designed from the literature review and the data collected by Blessmann (2011) for turbulent flow around cylinders.

Distribution of external pressure taps is illustrated in Figure 4. An upper perimeter line of pressure taps (1 to 24), a middle perimeter line of taps (25 to 48) and a lower perimeter line of taps (49 to 72) are located on the external surface of the model. Some pressure taps are located on the roof of the silo (top closure) but these pressure measurements will not be analyzed here.

Static pressures caused by wind on the model were measured in the table II of the test section (Figure 5). The mean and fluctuating pressures on the external surface of the model were obtained using static pressure taps and a Scanivalve 96-channel measurement system based on electronic pressure transducers. A numerical series of 9000 values with a

sampling frequency of 300 Hz was acquired at each measurement point and, subsequently, local pressure coefficients were determined for each pressure tap.

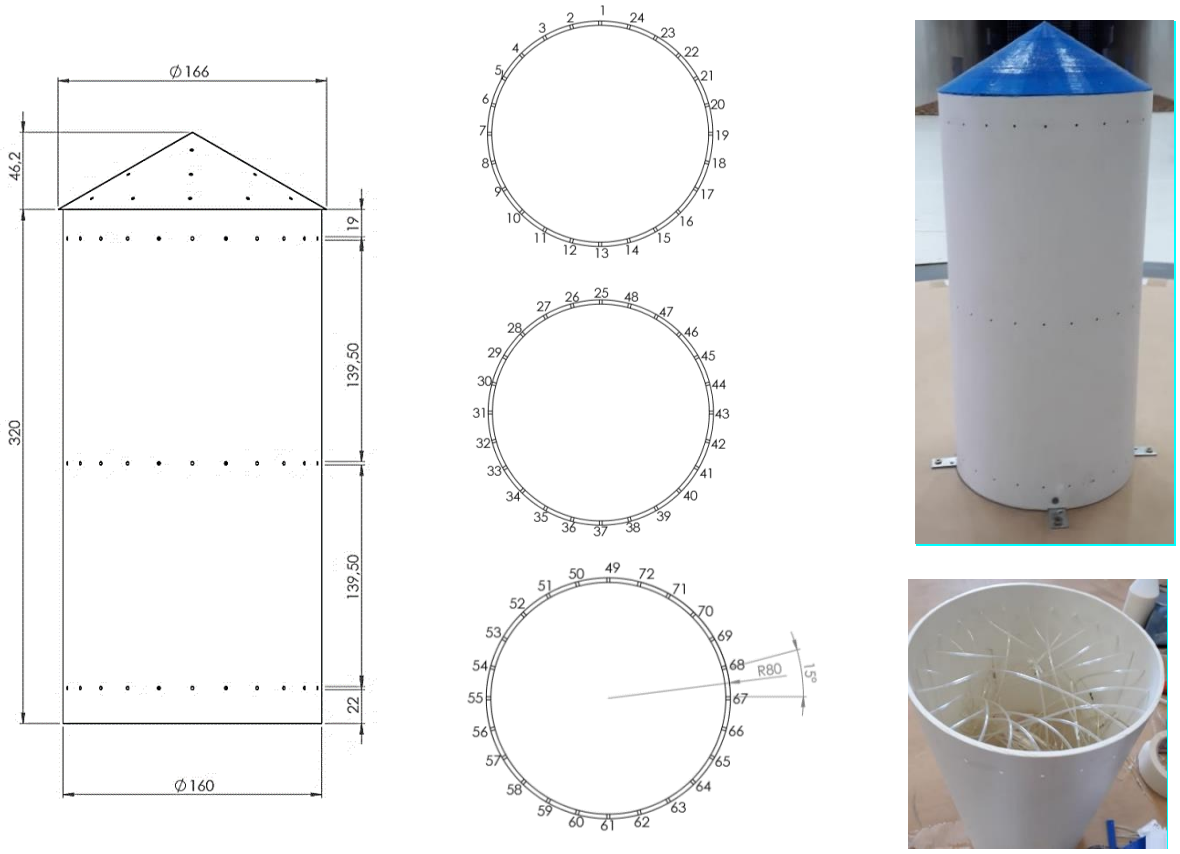

Figure 4. Distribution of the external pressure taps on the cylindrical surface and details of the smooth silo model.

Figure 5. Model instrumented in the wind tunnel test section and details of the rough surface silo model.

The tests were carried out with three different wind tunnel speeds in order to evaluate the effects of the variation of the Reynolds number on the pressure coefficients. Table 1 indicates the position of the regulator, the values of the mean velocity U and the Reynolds number Re for the measurements made. The Reynolds number is defined by the expression $Re = \rho UD/\mu$ where the characteristic length is the model diameter D. The density ρ and viscosity μ values correspond to the air flow during each test.

The roughness elements on curved surfaces modifies the Reynolds number effects on the values of the aerodynamic coefficients (Blessmann, 2011) and this type of behavior will be analyzed using the results of tests with smooth and rough models.

4. PRESSURE COEFFICIENT DISTRIBUTIONS

The local pressure coefficients were determined at 72 points on the cylindrical surface of the silo corresponding to each external pressure tap. The aerodynamic coefficients are dimensionless loads and the reference parameter used to obtain a pressure coefficient is the dynamic pressure q_z. The local mean pressure coefficient is defined by expression (1);

$$C_{p(m)} = \frac{\frac{1}{n}\sum_{i=1}^{n} \Delta p_i}{q_z} \tag{1}$$

the RMS value coefficient of local pressure (2) is

$$C_{p(RMS)} = \frac{[\frac{1}{n}\sum_{i=1}^{n} (p_i - p_m)^2]^{1/2}}{q_z} \tag{2}$$

and the peak (maximum and minimum) local pressure coefficients (3) are

$$C_{p(max)} = \frac{\Delta p_{max}}{q_z},\ C_{p(min)} = \frac{\Delta p_{min}}{q_z} \tag{3}$$

where Δp is the difference between the static pressure at measurement point (pressure tap on the surface) and the reference static pressure, q_z is the dynamic pressure measured at the reference height (maximum height of the silo model), n is the number of sampling values, p_m is the mean pressure, Δp_{max} and Δp_{min} are the maximum and minimum pressure values.

Table 1. Mean velocities and Reynolds numbers for wind tunnel tests.

Velocity regulator position	Mean velocity [m/s]	Reynolds number
4	11.00	1.14×10^5
5	14.00	1.45×10^5
8	21.10	2.07×10^5

Perimeter distributions of the mean, RMS and peak pressure coefficients in the upper, middle and lower line of pressure taps obtained by tests with a mean velocity of 11.00 m/s are shown in Figure 6. Mean pressure coefficient is Cp(m), RMS value coefficient is Cp(RMS), maximum peak coefficient is Cp(max) and minimum peak coefficient is Cp(min), while "smooth" indicate values obtained with smooth surface model and "rough" indicate values obtained with rough surface model. The peak pressure coefficient were obtained using absolute maximum and minimum values.

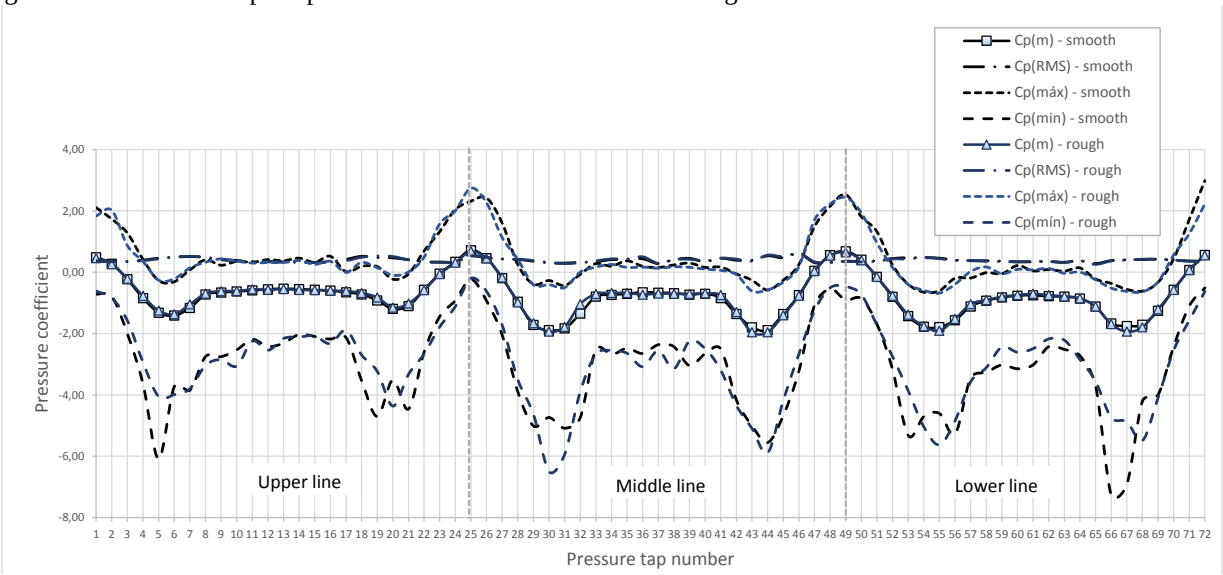

Figure 6. Distributions of the mean, RMS and peak pressure coefficients in the three perimeter lines of pressure taps obtained with a mean velocity of 11.00 m/s.

In the same way, distributions of the mean, RMS and peak pressure coefficients obtained using a mean reference velocity of 14.00 m/s are shown in Figure 7. Finally, distributions of pressure coefficients obtained by tests with a mean velocity of 20.10 m/s are shown in Figure 8. The general configuration of the distribution of coefficient values is maintained for the three test speeds.

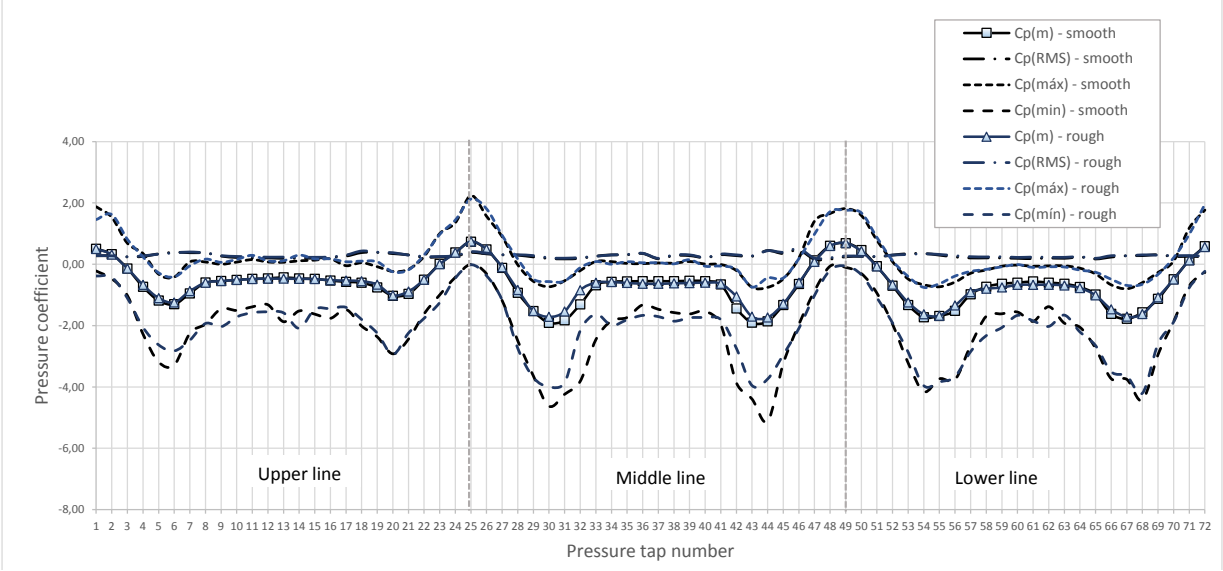

Figure 7. Distributions of the mean, RMS and peak pressure coefficients in the three perimeter lines of pressure taps obtained with a mean velocity of 14.00 m/s.

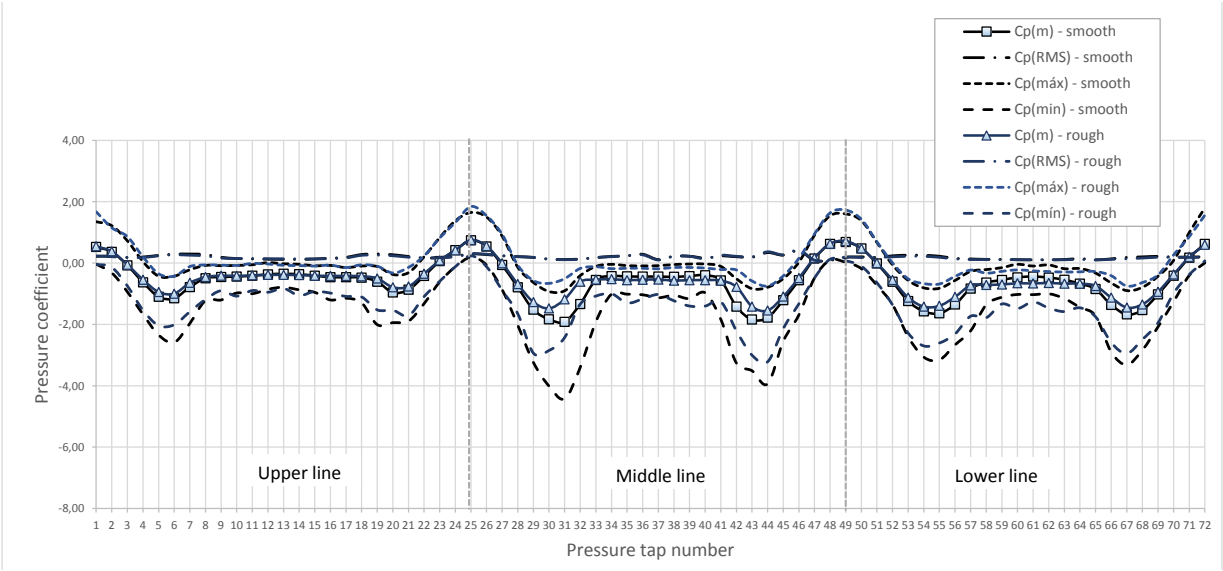

Figure 8. Distributions of the mean, RMS and peak pressure coefficients in the three perimeter lines of pressure taps obtained with a mean velocity of 20.10 m/s.

Some interesting behaviors are observed in the distributions of the pressure coefficients. The mean pressure distributions show very similar values for the smooth model and the rough model with the lowest test speed. Furthermore, it is possible to observe similar behaviors of the distributions obtained in the middle and lower perimeter lines, but the upper line shows less variations in mean pressure coefficients. The same comment can be made in relation to RMS values and maximum peaks, however, some differences are observed in the distribution of minimum peaks. The symmetry of the distributions in the three perimeter lines is widely verifiable except for the distribution of minimum peak values (Figure 6).

Distributions of the mean, RMS and peak pressure coefficients obtained with a mean velocity of 14.00 m/s are similar to those obtained with 11.00 m/s. However, small differences between smooth and rough model are evidenced in the

middle perimeter line for the mean pressure distribution. A great correspondence between the distributions of fluctuating pressure values obtained at 14.00 m/s with the smooth model and the roughness model is observed again except for the distribution of minimum peaks (Figure 7).

The mean pressure distributions obtained with 20.10 m/s for both models show greater differences than in the previous case, especially in the mean perimeter line. This behavior clearly indicates the displacement of the point of boundary layer detachment on the curved surface due to the increased roughness. Additionally, a decrease in the values of pressure fluctuations is observed as the velocity of the tests increases (Figure 8).

5. ANALYSIS OF THE TURBULENT ACTIONS

The displacement of the boundary layer detachment zone that is verified between smooth and rough model for the highest test velocity leads to further analysis of fluctuating pressures. Four measurement points (taps 25, 29, 31 and 37) on the middle perimeter line were selected. Point 25 corresponds to the windward front position of the model where the greatest positive pressure occurs. Points 29 and 31 are located in the boundary layer detachment zone where mean pressure differences occur between the values obtained with a smooth and rough model. Finally, point 37 located in the leeward position where the mean pressure indicates approximately constant negative values due to the suction wake.

Time pressure records of the four measurement points obtained at the speed of 20.10 m/s are shown in Figures 9 and 10 for smooth and rough model, respectively. Each record represents a digitized 30-second measurement with a sampling time Δt = 1/300 seconds, that is, each series has 9000 values. Records obtained with the smooth model indicate that the amplitude of the fluctuations is greater at points 29 and 31 located in the boundary layer detachment zone. Fluctuations decrease somewhat at windward point 25, and are still less at point 37 located on the leeward wake. Smaller amplitudes for points 29 and 31 are obtained with the rough model, that is to say, the “breakdown” of the greater turbulence scales is verified as a result of the elements of surface roughness.

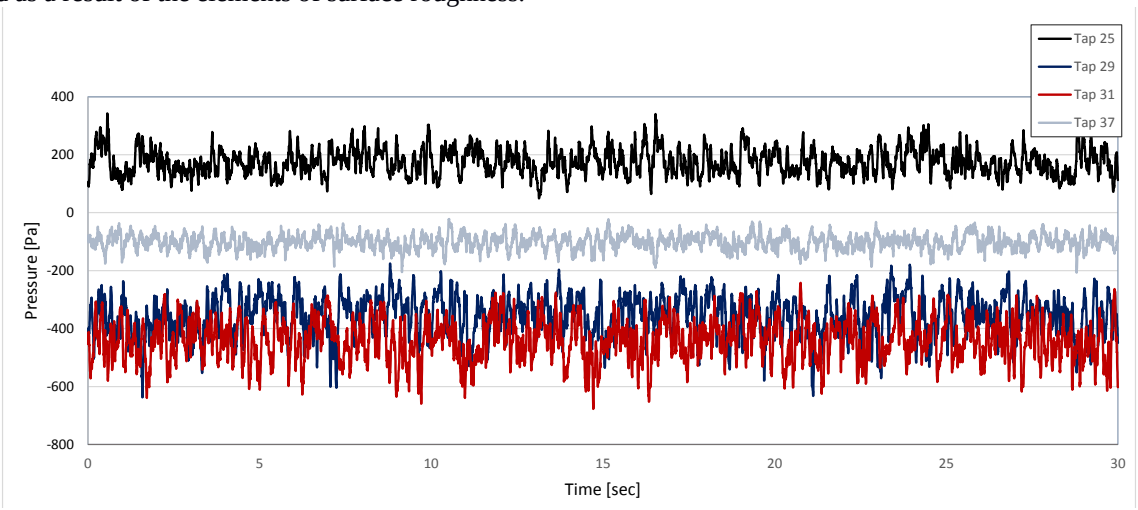

Figure 9. Pressure fluctuation records obtained with a mean velocity of 20.10 m/s for smooth model.

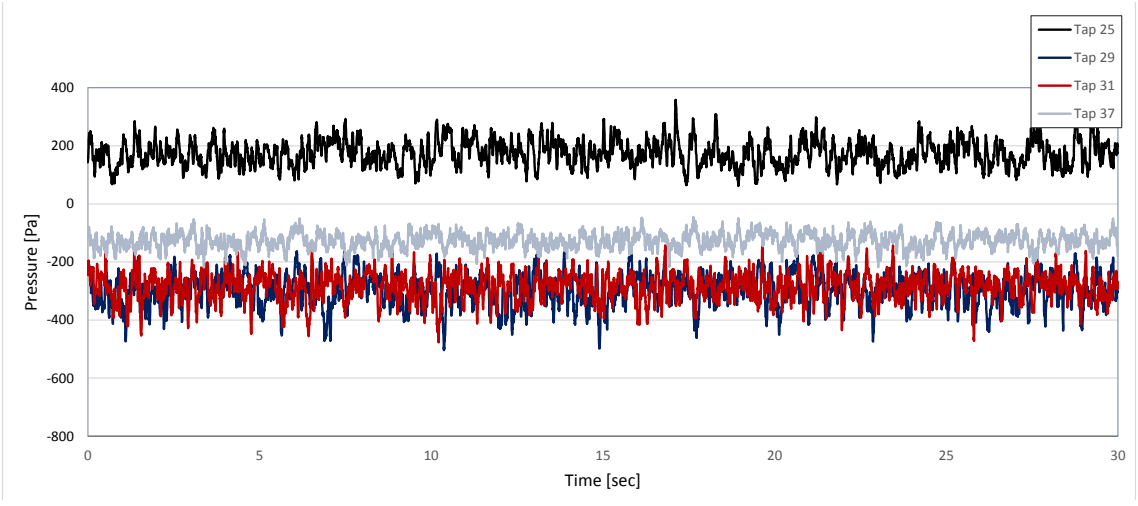

Figure 10. Pressure fluctuation records obtained with a mean velocity of 20.10 m/s for rough model.

The analysis in the time domain allows to visualize the fluctuation levels and the range of the maximum and minimum values, but it must be complemented with the analysis in the frequency domain. The functions of spectral density or spectrum of pressure fluctuations is obtained by means of a numerical algorithm based on FFT. Figure 11 shows the pressure spectra obtained for the previously selected points with the smooth and rough model, respectively.

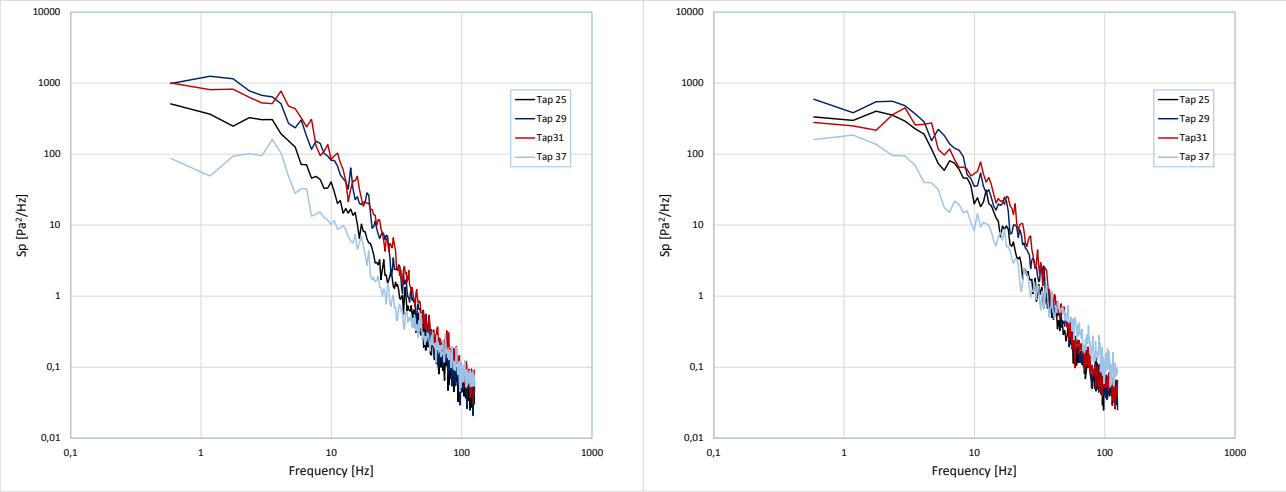

Figure 11. Pressure fluctuation Spectra obtained with a mean velocity of 20.10 m/s for smooth model (left) and rough model (right).

In general, it is not possible to verify the definition of highly correlated phenomena, that is, no areas of the spectrum are displayed that indicate energy concentrations of the vortices associated with a frequency or a small interval of frequencies. However, the spectral analysis allows verifying the effect of energy decrease associated with low frequencies at points 29 and 31, as well as an increase in energy levels at high frequencies for point 37, both effects in the case of the rough model. In general, it is observed a decaying tendency with a well-defined slope but the steepness of the slope varies slightly for the different pressure taps and also for both models. A more in-depth spectral analysis regarding this behavior should be performed. Only qualitative comparisons with spectra of velocity fluctuations have been carried out to date due to the limited amount of spectral studies with fluctuating pressures existing in the literature.

6. FINAL CONSIDERATIONS

The research work has the main objective of introducing fluctuating pressures and turbulence in the wind load analysis of these metallic structures. The preliminary results are very auspicious regarding the operation of the experimental device and also regarding the use of reduced-scale models. A great similarity of the distribution of RMS values and maximum peaks is observed in both models tested, even though absolute peak values were analyzed.

The symmetry of the distributions is verified extensively in each tap line and in both models. The analysis of the fluctuating pressures and the spectra obtained at the highest speed shows the effect of the roughness elements. An estimation of the drag coefficient as a function of the Reynolds number for both the smooth and rough surface models should be performed to complete the analysis of the results obtained in the tests.

The continuity of the research work will allow the effects of turbulence to be incorporated into the wind loads on these structures. The definition of wind gust duration times and their application to the statistical analysis of turbulent pressures will be the next step. It is also planned to experimentally evaluate the wind loads on groups of silos.

7. REFERENCES

Associação Brasileira de Normas Técnicas-ABNT, 1988. “Forças devidas ao vento em edificações”, NBR 6123. Rio de Janeiro, Brasil.

Blessmann, J., 1995. O vento na engenharia estrutural. Editora da Universidade/UFRGS, Porto Alegre, RS, Brasil.

Blessmann, J., 2011. “Aerodinâmica das Construções”. Editora da UFRGS, Porto Alegre, RS, Brasil.

De Bortoli, M., Natalini, B., Paluch, M. J. and Natalini, M. B.. 2002. “Part-Depth Wind Tunnel Simulations of the Atmospheric Boundary Layer”. *J. Wind Eng. Ind. Aerodyn.*, 90, pp. 281-291.

INTI, 2001. Centro de Investigación de los Reglamentos Nacionales de Seguridad para las Obras Civiles. CIRSOC 102: “Reglamento Argentino de Acción del Viento sobre las Construcciones”. Buenos Aires, Argentina.

Standen, N.M., 1972. “A Spire Array for Generating Thick Turbulent Shear Layers for Natural Wind Simulation in Wind Tunnels”, National Research Council of Canada, NAE, Report LTR-LA-94.

Wittwer, A. R., and Möller, S. V., 2000. “Characteristics of the low speed wind tunnel of the UNNE”. *J. Wind Eng. Ind. Aerodyn.*, V. 84 (3), pp. 307-320.